The Frequency Dependence of Bottom Trapping and its Implications for Gravity Current Interaction with Topography

Susan E. Allen

Department of Oceanography, University of British Columbia, Vancouver, British Columbia, Canada

Abstract. Experiments are discussed which clearly show a lack of coupling between surface gravity currents and dramatic topography. Contrasts are given with other baroclinic flows over topography. The frequency dependence of the vertical structure of topographically induced flow structures is reviewed. This concept can then be used to interpret the differences between the gravity experiments and the other baroclinic flows. Further limits on the types of flows which inhibit coupling between topography and surface layers are given using numerical modeling.

1 Introduction

Surface gravity currents generated by warm or fresh sources of water are common features of coastal regions (Norwegian Coastal Current, Leeuwin Current and the Vancouver Island Coastal Current). The interaction of these strongly nonlinear flows with underlying topography is of interest, particularly when one considers the strong interaction of coastally upwelled water with topography such as the streamers associated with the Mendocino Escarpment shown in Willmott (1984).

Following the study of Gill *et al.*, (1986) which investigated the effect of a step on a baroclinic current, experiments were performed to look at the effect of bottom topography on surface gravity currents and bores in a two layer fluid. The results were intriguing. There was basically no effect unless the surface layer directly interacted with the topography. These results contrasted sharply with the experiments of Gill *et al.*, (1986) and the later experiments of Allen (1988).

The next section will present the gravity current and bore experiments which will be contrasted with a number of baroclinic flows over topography from the literature in the following section. In section 4 linear theory will be invoked for a number of geometries to illustrate the frequency dependence of topographic coupling. Numerical simulations using flow over a canyon are used to put further limits on the flow conditions under which coupling will be inhibited. In the last section, an explanation and discussion linking all the results and explaining the lack of interaction of surface gravity currents and topography is given followed by a few conclusions.

2 Gravity Currents over Topography

2.1 Experimental Apparatus

The experiments were performed in a tank of dimensions 152.0 x 30.5 x 16.5 cm which was mounted on a 1 m diameter horizontal turntable which rotated counter-clockwise. For the first set of experiments a slab of styrofoam was wedged into the bottom of the tank, so that half the tank was 5 cm shallower than the other half. The second set of experiments incorporated a sharp ridge of height 7 cm and width 1.5 cm completely dividing the tank into two sections. The Coriolis parameter, f, was varied from 0.26 to 1.3 s^{-1}. The tank was filled to a height of H = 6.5 to 11 cm and salt was added to increase the density to give a reduced gravity (with respect to fresh water) of g' = 3.3 to 9 cm s^{-2}. For some experiments, a fresh water layer of depth h_2 = 1 to 2 cm was floated on top of the salt water. A dam was inserted into one end of the tank and fresh, dyed water was carefully floated onto the salt water in the manner of Stern *et al.* (1982) and Griffiths and Hopfinger (1983). The depth, h_1, of fresh water behind the dam varied from 2.5 to 6 cm and the length, ℓ, of the fresh water region was varied from 17 to 25 cm. A full list of the experimental parameters is given in Tables 1 and 2.

The experiment was started by removing the dam. The ensuing current was photographed both from above and the side (using a 45 degree mirror). By including a clock in the field of view, measurements of the speed of the current could be made.

2.2 Results

As the dam is pulled the fresh water flows out over the salt water. However, within an inertial period, the flow is turned to the right by the Coriolis force. Where the flow meets the wall, a gravity current is formed which flows down the tank, hugging the right-hand wall. The properties of rotating gravity currents (in the absence of topography) are described by Stern *et al.* (1982) and Griffiths and Hopfinger (1983).

The gravity current travels down the right hand wall until it reaches the topography. Unless the gravity current hits the topography, the current itself is unaffected by the topography. That is, no dyed fluid crosses the tank at the topography and the

Table 1: Experimental Parameters for Gravity Currents over a Step

#	ℓ (cm)	f (s^{-1})	g (cm s^{-1})	h_1 (cm)	h_2 (cm)	H (cm)
1	(15.0 ± 0.5)	(1.06 ± 0.02)	(5.7 ± 0.1)	(5.0 ± 0.3)	0.	(10.0 ± 0.2)
2	(15.0 ± 0.5)	(1.08 ± 0.04)	(5.6 ± 0.1)	(5.0 ± 0.3)	0.	(11.2 ± 0.2)
3	(15.0 ± 0.5)	(1.06 ± 0.02)	(4.9 ± 0.1)	(5.0 ± 0.3)	0.	(11.4 ± 0.1)
4	(17.5 ± 0.5)	(1.03 ± 0.02)	(8.2 ± 0.1)	(5.2 ± 0.3)	0.	(10.0 ± 0.2)
5	(17.5 ± 0.5)	(1.05 ± 0.02)	(7.6 ± 0.1)	(5.0 ± 0.3)	0.	(8.5 ± 0.2)
6	(27.0 ± 0.5)	(1.06 ± 0.02)	(7.0 ± 0.1)	(4.9 ± 0.3)	0.	(8.5 ± 0.2)
7[1]	(20.5 ± 0.3)	(1.05 ± 0.02)	(9.0 ± 0.1)	(2.6 ± 0.4)	0.	(9.3 ± 0.2)
8	(22.5 ± 0.3)	(1.02 ± 0.02)	(6.5 ± 0.1)	(5.0 ± 0.5)	0.	(11.9 ± 0.2)
10	(21.6 ± 0.2)	(1.04 ± 0.02)	(8.1 ± 0.1)	(4.5 ± 0.4)	0.	(9.6 ± 0.1)
11	(22.2 ± 0.2)	(1.02 ± 0.02)	(7.9 ± 0.1)	(4.9 ± 0.3)	(1.0 ± 0.3)	(10.2 ± 0.1)
13	(19.2 ± 0.2)	(0.262 ± 0.001)	(3.5 ± 0.1)	(3.6 ± 0.2)	0.	(10.0 ± 0.2)
14	(24.8 ± 0.2)	(0.266 ± 0.001)	(3.3 ± 0.1)	(3.6 ± 0.2)	0.	(8.0 ± 0.2)
15	(22.0 ± 0.3)	(1.02 ± 0.02)	(6.4 ± 0.1)	(5.1 ± 0.3)	0.	(7.0 ± 0.2)
16	(23.6 ± 0.2)	(1.07 ± 0.02)	(5.7 ± 0.1)	(5.1 ± 0.2)	0.	(6.5 ± 0.1)
17	(17.0 ± 0.1)	(0.359 ± 0.003)	(4.3 ± 0.1)	(4.0 ± 0.2)	(2.0 ± 0.2)	(10.0 ± 0.1)
18	(17.4 ± 0.1)	(0.510 ± 0.002)	(4.0 ± 0.1)	(4.0 ± 0.2)	(1.0 ± 0.2)	(10.1 ± 0.1)
19	(17.1 ± 0.1)	(0.515 ± 0.002)	(4.1 ± 0.1)	(4.4 ± 0.2)	(1.0 ± 0.2)	(10.0 ± 0.1)
20	(17.1 ± 0.1)	(0.532 ± 0.002)	(4.1 ± 0.1)	(4.5 ± 0.2)	(1.5 ± 0.2)	(10.1 ± 0.1)
21	(17.0 ± 0.1)	(1.05 ± 0.01)	(4.1 ± 0.1)	(5.0 ± 0.3)	(2.0 ± 0.2)	(10.0 ± 0.1)
22	(17.2 ± 0.2)	(0.528 ± 0.002)	(4.1 ± 0.1)	(6.0 ± 0.3)	(3.0 ± 0.2)	(10.0 ± 0.1)
23	(17.0 ± 0.1)	(0.517 ± 0.002)	(4.1 ± 0.1)	(3.0 ± 0.3)	0.	(10.0 ± 0.1)
24	(17.2 ± 0.1)	(0.526 ± 0.002)	(4.1 ± 0.1)	(4.0 ± 0.3)	0.	(10.0 ± 0.1)
25	(17.1 ± 0.1)	(0.519 ± 0.002)	(4.2 ± 0.1)	(5.0 ± 0.3)	(2.0 ± 0.2)	(9.9 ± 0.1)
26	(17.1 ± 0.1)	(0.519 ± 0.002)	(4.1 ± 0.1)	(3.9 ± 0.2)	(1.0 ± 0.2)	(10.0 ± 0.1)
27	(17.0 ± 0.1)	(0.521 ± 0.002)	(4.1 ± 0.1)	(5.0 ± 0.2)	(2.0 ± 0.2)	(10.0 ± 0.1)
28	(17.4 ± 0.1)	(0.517 ± 0.002)	(4.1 ± 0.1)	(4.1 ± 0.2)	0.	(10.0 ± 0.1)
29	(17.2 ± 0.1)	(0.535 ± 0.002)	(3.9 ± 0.1)	(5.0 ± 0.2)	(2.0 ± 0.2)	(10.3 ± 0.1)
30	(16.9 ± 0.1)	(0.536 ± 0.002)	(4.2 ± 0.1)	(4.0 ± 0.3)	(1.0 ± 0.2)	(9.8 ± 0.1)
31	(16.8 ± 0.1)	(0.528 ± 0.002)	(3.7 ± 0.1)	(3.3 ± 0.2)	0.	(10.0 ± 0.1)
32	(17.1 ± 0.2)	(1.31 ± 0.01)	(8.3 ± 0.1)	(3.0 ± 0.3)	0.	(10.0 ± 0.1)
33	(17.4 ± 0.1)	(0.519 ± 0.002)	(4.1 ± 0.1)	(3.2 ± 0.2)	0.	(10.0 ± 0.1)

[1] The gravity current started in the shallow water and flowed over the step into deeper water.

Table 2: Experimental Parameters for Gravity Currents over a Ridge

#	ℓ (cm)	f (s^{-1})	g (cm s^{-1})	h_1 (cm)	h_2 (cm)	H (cm)
38	(17.0 ± 0.1)	(0.528 ± 0.002)	(4.0 ± 0.1)	(5.0 ± 0.3)	(2.0 ± 0.2)	(7.3 ± 0.1)
39	(17.1 ± 0.1)	(0.535 ± 0.002)	(6.2 ± 0.1)	(5.0 ± 0.3)	(2.0 ± 0.2)	(7.0 ± 0.1)
42	(17.2 ± 0.1)	(0.526 ± 0.002)	(6.0 ± 0.1)	(5.0 ± 0.2)	(2.0 ± 0.2)	(8.0 ± 0.1)
43	(17.2 ± 0.1)	(0.528 ± 0.002)	(6.0 ± 0.1)	(4.1 ± 0.2)	0.	(8.0 ± 0.1)
44	(17.0 ± 0.1)	(0.532 ± 0.002)	(6.0 ± 0.1)	(4.1 ± 0.2)	0.	(9.0 ± 0.1)
45	(17.3 ± 0.1)	(0.532 ± 0.002)	(6.0 ± 0.1)	(4.0 ± 0.2)	0.	(10.0 ± 0.1)
46	(17.3 ± 0.1)	(0.524 ± 0.002)	(6.0 ± 0.1)	(4.0 ± 0.2)	0.	(11.0 ± 0.1)
47	(17.2 ± 0.1)	(0.530 ± 0.002)	(6.0 ± 0.1)	(5.0 ± 0.2)	(2.0 ± 0.2)	(8.0 ± 0.1)
48	(17.0 ± 0.1)	(0.526 ± 0.002)	(6.1 ± 0.1)	(5.0 ± 0.2)	(2.0 ± 0.2)	(9.0 ± 0.1)
49	(16.8 ± 0.1)	(0.539 ± 0.002)	(6.0 ± 0.1)	(5.0 ± 0.2)	(2.0 ± 0.2)	(10.0 ± 0.1)
50	(17.5 ± 0.1)	(0.535 ± 0.002)	(6.0 ± 0.1)	(4.0 ± 0.2)	0.	(7.5 ± 0.1)

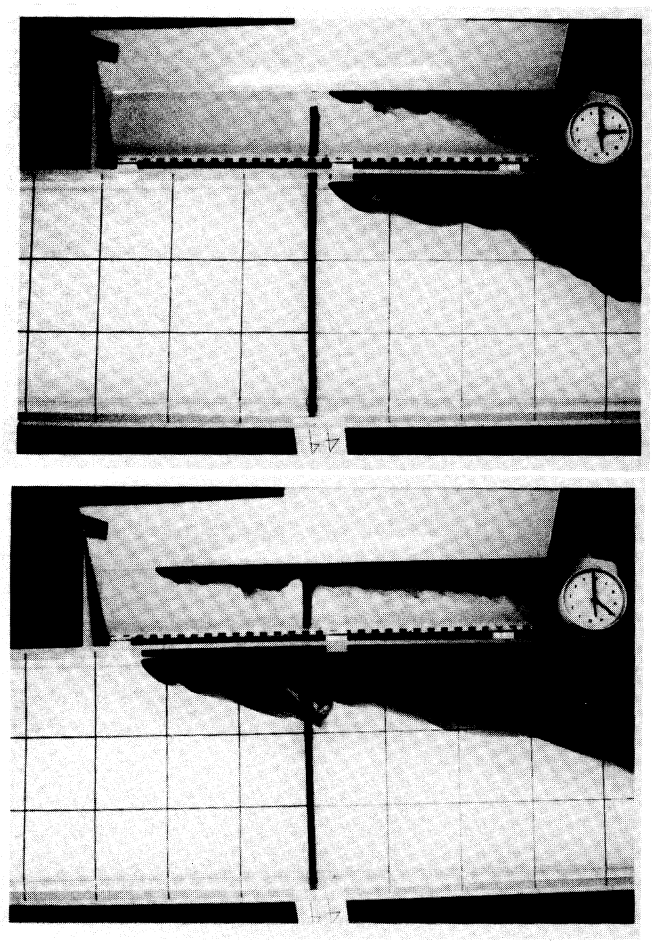

Figure 1: Figure showing a gravity current a) approaching and b) passing over a ridge. The top part of each frame shows a side view whereas the lower part of the frame is from above. The marked squares are 10 cm x 10 cm. Only the centre part of the tank is shown. See Table 2 for parameters; this is experiment 44.

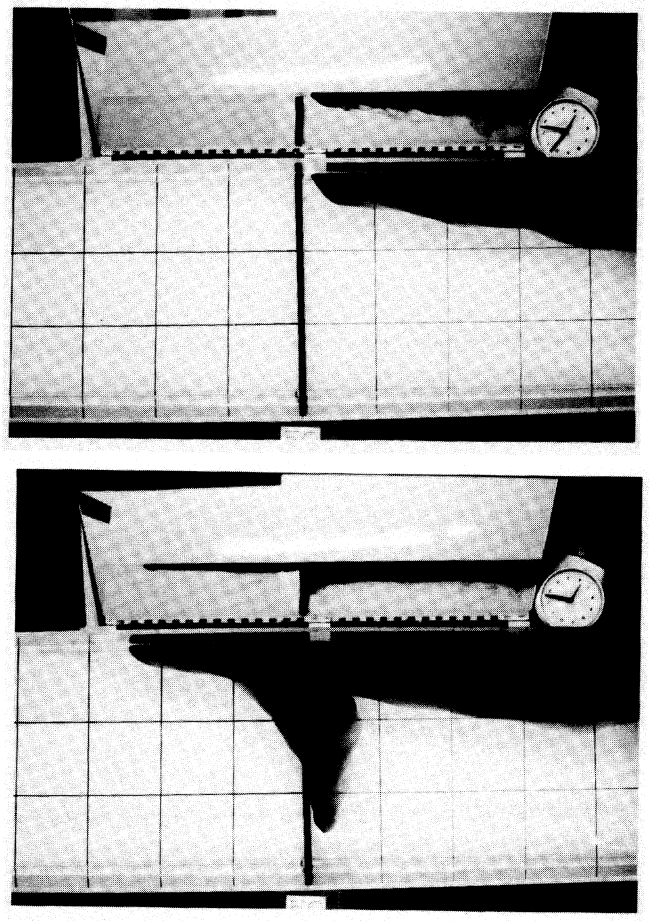

Figure 2: Figure showing a gravity current a) approaching and b) bifurcating over a ridge. See Figure 1 for details of the field of view. See Table 2 for parameters; this is experiment 50.

speed, depth and width of the gravity current remains the same (within measurement limits) as the current crosses the topography. An example, showing the current approaching and passing over a ridge, is given in Figure 1.

In the absence of topography the gravity current generates a return flow in the deep water which is broad (stretches across the tank) and is about 1/5th as strong as the current itself (Allen and Allen, 1995). Thus, the deep water flow must be affected by the topography; it is only the surface gravity current which is unaffected.

Occasionally an eddy formed at the step after the passage of the head. This eddy would tend to move fluid across the tank. However, it was not the only eddy to form and not necessarily the largest.

Deep water movement was observed under the gravity current, towards the barrier region. A deep current forms over the step in the two layer case running across the step away from the approaching bore. A sketch is given in Figure 3. This current is stronger for deeper original surface layers. Generally, this current forms after the current has traversed the step.

If the current actually hit the topography, a secondary current formed which crossed the tank, generally to the left of the topography. Occasionally it would stray over the step and cross at as much as a 45 degree angle. The original current continued with reduced size and speed. An example showing a gravity current hitting the ridge and bifurcating is shown in Figure 2. In a two layer fluid. the cross tank current usually took the form of a series of eddies. In the case of the step and a two layer fluid, an eddy formed where the current hit the jet and cross tank current/eddies formed out of this eddy. Examples for the two layer fluid are shown in Figure 4 and Figure 5.

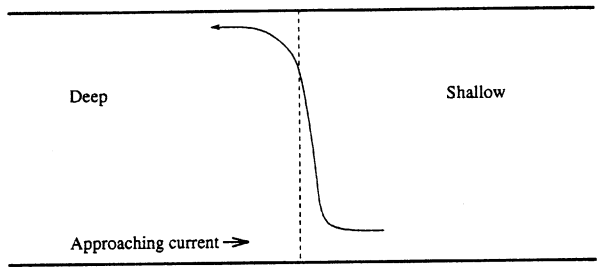

Deep, return current, over a step

Figure 3: Figure showing, from above, the deep return current seen over a step for a two layer fluid. The direction of the approaching bore is marked.

3 Other Baroclinic Flows over Topography

The lack of effect of a dramatic piece of topography is not common. This section presents three examples where topography strongly affects surface layers not in contact with it.

3.1 Two layer geostrophic flow over a Step or Slope

The experiments described in Gill *et al.*, (1986) and Allen (1988) consider geostrophic flow forced over a step and slope respectively. The step was identical to the one described above. The slope was 4 cm high and 8 cm long. In both cases the flow was forced by placing a barrier *along* the wall, across the topography. In each case distinct cross tank flow at the topography is seen. An example of a numerical solution is shown in Figure 6. Note the flow out along the topography at the bottom on the slope and the flow towards the wall at the bottom. These along-slope flows are in the same sense as those in the lower layer even though the along-wall flows are in opposite directions (Allen, 1988).

3.2 Eddy experiments

Consider a circular tank mounted on a rotating table and initially containing a homogeneous fluid at rest. If a constant flux of buoyant water is introduced away from the tank walls a circular anti-cyclonic eddy will form (Griffiths and Linden, 1981). If this is done over a sloping bottom, the eddy elongates in a direction which keeps the shallow water to the right (in the direction topographic Rossby waves propagate). If the eddy is unstable, it breaks up into a string of eddies and each eddy propagates across the tank, again in the direction which keeps the shallow water on the right (Linden, 1991; Davey and Killworth, 1989). Thus, although the eddy is a surface phenomena, it directly feels the bottom topography.

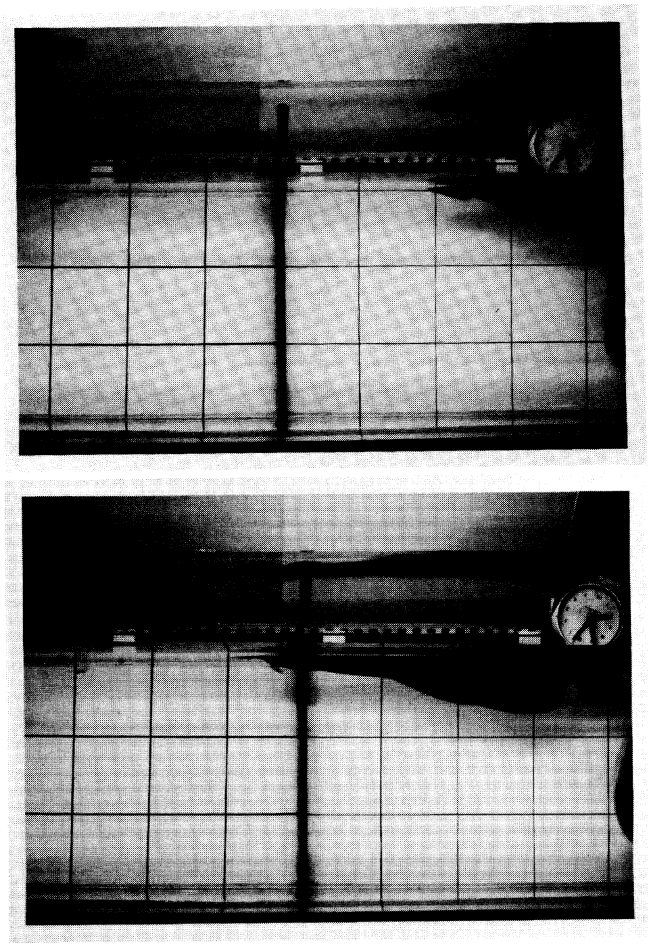

Figure 4: Figure showing a gravity current a) approaching and b) crossing over a ridge. See Figure 1 for details of the field of view. See Table 2 for parameters; this is experiment 42.

Davey and Killworth (1989) give an analytic solution for the similar β-plane problem assuming the lower layer is quiescent. In the laboratory case however, the lower layer must move as that is the only way the upper layer could "feel" the bottom topography (unlike the β effect). If one follows Davey and Killworth's arguments but considers a barotropic solution (ignoring the density difference between the two fluids) one gets the same flow pattern as they derived for the linear baroclinic flow. Under the source itself, the flow is towards the deeper water ("south") whereas "west" of the north half of the source, the flow is towards the source and "west" of the south half of the source, the flow is away from the source. This derived, linear flow pattern is three quarters of an elongated anti-cyclonic vortex stretching out to the west of the source.

3.3 Ridge

Experiments conducted in Grenoble by D. Renouard (Allen *et al.*, 1995) investigated barotropic tidal flow over a long bank or ridge in a two layer fluid. To gener-

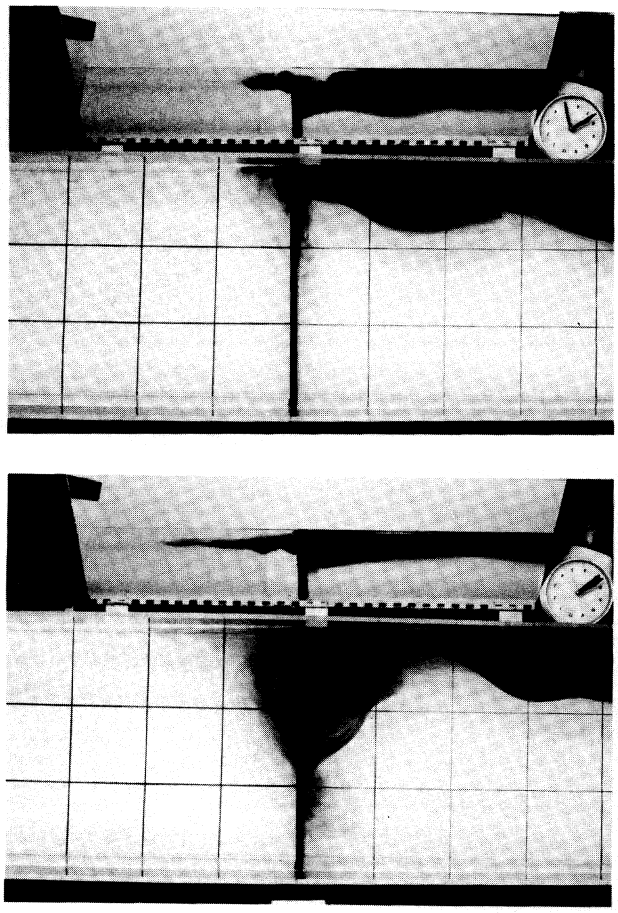

Figure 5: Figure showing a bore a) approaching and b) splitting over a ridge. See Figure 1 for details of the field of view. See Table 2 for parameters; this is experiment 39.

ate the tides, the ridge was oscillated. Measurements were made in the centre of the ridge of the velocity in each layer. The frequency of oscillation of the ridge, ω and the period of rotation $4\pi/f$ were varied. A number of experiments were performed (Germain and Renouard, 1991) but I will discuss only two examples here.

The ridge is 30 cm high and 4 m long. The lower layer is 40 cm deep, the upper layer is 4 cm deep and the reduced gravity between the two layer is 6.5 cm s^{-2}. Thus, the ridge is 3/4 of the depth of the lower layer and the topography can be classified as large. The ridge was oscillated back and forth 30 cm.

For the first, a weakly rotating case, $\omega/f = 0.67$. The lower layer velocity has an amplitude of 5.5 cm/s in the cross-ridge direction and about 1 cm/s in the along ridge direction. The upper layer velocities are 2 cm/s across and about 1 cm/s along the ridge. Contrast these values with a strongly rotating case, $\omega/f = 0.14$. The lower layer velocities are 5 cm/s and 4 cm/s across and along the ridge but the upper layer velocities are almost as strong at 3.5 cm/s across and 3 cm/s along.

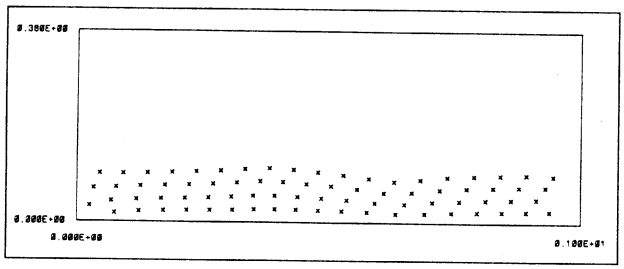

Figure 6: Figure showing movement of tracers in a numerical simulation of the Allen (1988) experiments. The fluid is stratified, with the upper layer deeper near the wall initially. The tracers mark the upper layer inside the barrier. Note the movement out across the tank. Depth of upper layer 14.4 cm, depth of lower layer 7.9 cm, reduced gravity 4.24 cm s^{-2}, barrier 5.1 cm from the wall.

Thus at a high, although still subinertial, frequency there is weak coupling whereas at a much lower frequency the upper layer flows are almost as strong as the lower layer flow.

4 Linear theories of the vertical height of topographic effects

4.1 Steady Flow

In Hogg (1973) steady, low Rossby number stratified flow over a circular cylinder is considered. If the fluid is homogeneous, by the theory of Taylor and Proudman, a Taylor column will form over the cylinder and no streamlines from off the cylinder will penetrate the area over the cylinder. If the fluid is stratified, such behaviour is limited in vertical extent over the body. Hogg's theory gives the height to which a Taylor cone will exist in a stratified fluid, over a circular body, as L^2/R^2 times the height of the body, where L is the radius of the body and R is the internal Rossby radius.

In the flows considered here, the width of the topography is much greater than the width of the background current. Assuming that in this case the appropriate lengthscale is the lengthscale of the current, all flows in sections 2 and 3 have L^2/R^2 of approximately one. Thus, if these flows were steady (they are not) and of low Rossby number (they are not), they all should show topographically influenced flow right to the surface.

4.2 Oscillatory Flow

Rhines (1977) presents a coherent picture of subinertial waves trapped over a sloping bottom (his fast baroclinic waves). These topographic Rossby waves are trapped with a depth $f\lambda/N$ of the bottom for wavelengths of order of or smaller than the internal Rossby radius. The symbols f, λ and N represent the Coriolis frequency, one over the wavenumber, and

the Brunt-Väisälä frequency, respectively. For longer wavelengths the flow is barotropic.

If one considers the topographic waves which travel along a simple linear slope between two flat basins (as would be appropriate for the slope geometry of sections 2 and 3) the dispersion relation has a similar form to that for β-plane Rossby waves. Long waves are non-dispersive; at some intermediate wavenumber the group speed goes to zero and thereafter the frequency decreases with wavenumber. For two layer flow over a slope, those waves having wavelengths of approximately one internal Rossby radius have the highest frequencies (group speed near zero).

Thus higher frequency motions are bottom trapped whereas long wavelength, low frequency motions are felt throughout the water column. Note that Rhines' theory is for low Rossby number and infinitely wide topography.

5 Discussion

Interpretation of the oscillating ridge experiments, section 3.3, follows directly from Rhines (1977) assuming 1) the nonlinear nature of the flow is not important in determining its vertical scale and 2) forced waves behave similarly to free waves. The fast subinertial frequency excites bottom trapped topographic waves whereas the slower frequency excites long, almost barotropic Rossby waves. For these forced waves, the wavelength is the length of the ridge, N is approximately $(g'/H)^{1/2}$ where H is the depth of the upper layer. This gives trapping within 4 cm of the ridge for the high frequency, low rotation rate flow which would imply little effect in the upper layer as is observed. For the low frequency, high rotation rate flow the wavelength is much greater than Rossby radius and as expected the effect of the ridge is strong in the upper layer.

The eddy experiments are forced slowly. Fluid is added over many inertial periods. Thus the frequency of the forcing is low and it has barotropic as well as baroclinic character (fluid is not removed from the lower layer so the forcing is not purely baroclinic). This type of forcing leads to the generation of low frequency, long wavelength topographic waves. Invoking Rhines' theory, and again assuming the nonlinearity is not important to the vertical structure, these waves should be nearly barotropic. Thus the surface flow is strongly affected by the bottom topography in this case.

The step and slope experiments with the barrier placed along the topography are also forced relatively slowly. Although the dam break is sudden, the initial response is flow parallel to the topographic contours. Only as the flow turns due to the Coriolis force does it "feel" the topography. Thus the frequency scales of the forcing of the topographic waves are fairly low. As is observed, these waves have near barotropic behaviour and the surface flow is affected by the topography.

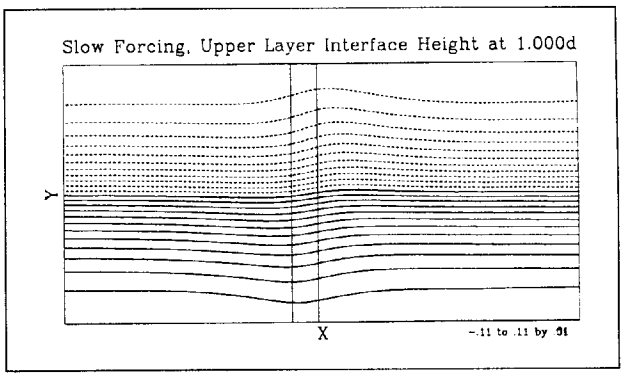

Figure 7: Figure showing a the surface elevation one day after forcing began. The contour levels are in metres. The domain is 240 km by 120 km and the position of the canyon is marked. The surface layer is 50 m deep and the lower layer is 200 m deep in the canyon, 100 m deep over the shelf. The reduced gravity between the two layers is 0.1 m s^{-2}.

In the surface gravity current experiments, on the other hand, the current topography interaction is quite quick. The subinertial frequencies generated are close to f and these waves are bottom trapped. Thus currents at the topography are seen in the lower layer but the upper layer is unaffected by the topography.

6 Complications due to wavelength

Numerical and analytic modelling (Allen, 1995) has considered multi-layer flow over a canyon. Here we will consider two layers where the lower layer is in contact with the topography but the upper layer lies above. The flow is forced by assuming that wind forcing generates an Ekman layer which, through Ekman pumping, removes water from the main fluid column over the shelf. The Ekman layer is not modeled and the Ekman pumping is modeled as a sink. Simplifying the problem further, here we neglect the shelf break.

The wind is assumed to start at zero and linearly increase in intensity over one half of an inertial period. Thereafter it decreases linearly in intensity. The surface elevation (which approximates the upper layer streamlines) after one day (about 1.4 inertial periods) is shown in Figure 7. The effect of the canyon is clearly visible with along canyon, down pressure, flow generated within the canyon.

To consider the fast introduction of topography, a case with a flat bottom was forced in the same way as above. After one day, a canyon was suddenly added. The lower layer flow in the canyon was reduced to conserve momentum and match the flux across the canyon walls. The surface elevation is shown in Figure 8 one day after the canyon was introduced (two days after the start of the flow). The surface flow is similar to

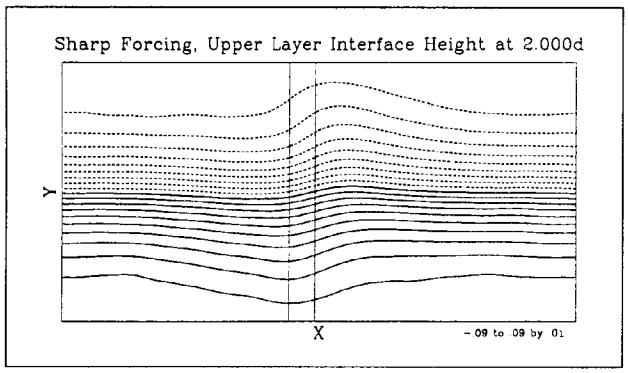

Figure 8: Figure showing the surface elevation one day after a canyon was introduced; see text. Other parameters as in Figure 7.

the gently forced case and is strongly affected by the topography. The pattern is noisier because the sharp introduction of the canyon generates Poincaré waves.

This numerical experiment illustrates that the frequency of the forcing is not the sole mechanism for determining the wavelength and frequency of the topographic waves. At the time the canyon is introduced, the surface and interface elevation change from high to low values along the canyon. Thus the wavelengths of the topographic Rossby waves which travel along the canyon (Chen and Allen, 1995) are of order of the Rossby radius up to half the size of the domain. The long waves are primarily barotropic (assuming Rhines' (1977) theory holds) and so the surface flow is influenced by the topography.

Various numerical complications make it difficult to consider the unrealistic case of flow over a canyon near the wall. Consider again the experiments. The width of the gravity current and the flow set up by the barrier along the wall were similar as the barrier was placed, in some cases, closer than a Rossby radius to the wall. In this case frequency of forcing, not the initial along-topography wavelength, gives an explanation.

7 Conclusions

Linear theory (Hogg, 1973 and Rhines, 1977) gives the basis for determining the vertical scale of topographic influence. Nonlinear effects do not seem to be important. From the type of forcing and the geometry, the frequency and wavelength of the topographic Rossby waves is estimated and compared to the Rossby radius. Provided short wavelength, high frequency waves are generated the flow is confined to $\lambda f/N$ of the bottóm. Lower frequency, long waves are expected to follow the Hogg limit of L^2/R^2H.

The above explanation was applied to the laboratory results for gravity currents over steps and slopes, eddies over a slope, oscillatory flow over a ridge, and the numerical results for wind driven flow over a canyon.

References

Allen, M. C. and S. E. Allen, 1995: Beyond $(g'h)^{1/2}$, the speed of rotating gravity currents. In preparation.

Allen, S. E. 1988: *Rossby adjustment over a slope.* PhD thesis, University of Cambridge, 206 pp.

Allen, S. E. 1995: Topographically generated, subinertial flows within a finite length canyon. Submitted to *J. Phys. Oceanogr.*

Allen, S. E., D. P. Renouard, and J.-M. Baey, 1995: Currents and internal waves generated by periodic flow over topography. In preparation.

Chen, X. and S. E. Allen, 1995: Influence of canyons on shelf currents – a theoretical study. Submitted to *J. of Geophys. Res.*

Davey, M. K. and P. D. Killworth, 1989: Flows produced by discrete sources of buoyancy. *J. Phys. Oceanogr.* **19**, 1279–90.

Germain, J.-P. and D. Renouard, 1991: On permanent nonlinear waves in a rotating fluid. *Fluid Dyn. Res.* **7**, 263–278.

Gill, A. E., M. K. Davey, E. R. Johnson, and P. F. Linden, 1986: Rossby adjustment over a step. *J. Marine Res.* **44**, 713–738.

Griffiths, R. W. and E. J. Hopfinger, 1983: Gravity currents moving along a lateral boundary in a rotating fluid. *J. Fluid Mech.* **134**, 357–399.

Griffiths, R. W. and P. F. Linden, 1981: The stability of buoyancy-driven coastal currents. *Dyn. Atmos. Oceans* **5**, 281–306.

Hogg, N. G. 1973: On the stratified Taylor column. *J. Fluid Mech.* **58**, 517–537.

Linden, P. F. 1991: Dynamics of fronts and eddies. In Osborne, A., editor, *Nonlinear topics in ocean physics* Int. School of Physics, "Enrico Fermi". North Holland.

Rhines, P. B. 1977: The dynamics of unsteady currents. In Goldberg, E. D., I. N. McCave, J. J. O'Brien, and J. M. Steele,, editors, *The Sea. Volume 6: Marine Modelling.* John Wiley & Sons.

Stern, M. E., J. A. Whitehead, and B.-L. Hua, 1982: The intrusion of a density current along the coast of a rotating fluid. *J. Fluid Mech.* **123**, 237–265.

Willmott, A. J. 1984: Forced double Kelvin waves in a stratified ocean. *J. Marine Res.* **42**, 319–358.